Error analysis and modelling of double saturating exponential dose response curves from SAR OSL dating

G.W. Berger [1] and R. Chen [2]

[1] Desert Research Institute, 2215 Raggio Parkway, Reno, NV 89512, USA.
(e-mail: glenn.berger@dri.edu)
[2] School of Physics and Astronomy, Tel-Aviv University, Tel-Aviv, 69978, Israel

(Received 14 March 2011; in final form 28 April 2011)

Abstract

Increasingly observed in single-aliquot regenerative dose (SAR) optically stimulated luminescence (OSL, also termed photon stimulated luminescence or PSL) dating studies of sedimentary quartz are dose response curves that at high doses are not satisfied by a single saturating exponential (SSE) regression model. Commonly these can appear to be satisfied by a SSE+Linear (E+L) regression model, but some authors have proposed that a double saturating exponential (DSE) model would more closely fit the observed dose response curves (DRCs), especially in the region of highest applied doses. As error analysis for SAR equivalent dose (D_e) values derived from a DSE model is not yet available through the widely available Risø supplied software (Analyst), we present here a regression and error analysis scheme for DSE SAR data, and also a simple charge traffic model that generates approximate DSE dose responses. To illustrate results from our error analysis, we employ two SAR high dose data sets for fine-grain quartz, and compare graphically the SSE, E+L and DSE fits for each data set. These comparisons show clearly that such data are more closely fitted by a DSE regression than by the other two models. This result, and the charge traffic model, lend validity to the physical reality of DSE regression models, and have implications for quartz SAR dating of older sediments.

Introduction

Recently there has been increasing interest in the use of the high dose part of quartz SAR DRCs to estimate burial ages from unheated sediments (e.g., Lowick and Preusser, 2011; Lowick et al., 2010a, 2010b; Murray et al., 2007, 2008; Pawley et al., 2008, 2010; Timar et al., 2010). Most of these reports are concerned with how to assess the accuracy of equivalent dose (D_e) values derived from such DRCs because some of the age estimates are lower than expected based on indirect, independent evidence. Although these studies considered several possible explanations for the observed age estimate discrepancies (e.g. validity of independent ages, accuracy and/or variation of estimates of past water concentration, soundness of SAR self-consistency tests), part of the discussion in these reports of high-dose DRCs concerns the best-fit model, though the examples of age underestimations illustrated by, for example, Lowick and Preusser (2011) do not depend on the fitting model.

Berger (2010) summarized several published reports of high dose TL (thermoluminescence) and SAR DRCs that appeared to be best fitted by an E+L regression model. Additional examples of high dose SAR DRCs that appeared to be best fitted by an E+L model are reported in chapter 5 of Bøtter-Jensen et al. (2003). All of these examples used relatively few dose points and did not extend the DRC to very high (many kGy) doses. Berger (2010) noted that some authors (Wintle and Murray, 2006; Murray et al., 2007, 2008) considered that a DSE model would also fit their DRCs. Recently, Lowick and Preusser (2011), Lowick et al. (2010a), and Pawley et al. (2010) showed that a DSE model would fit some of their DRCs as well as an E+L model up to applied doses of ~1 kGy. These authors used the E+L model to calculate interpolated D_e values from the high dose region of the relevant DRCs because an interpolation and error analysis scheme for calculation of D_e values from a DSE model was not available to them.

We present here a regression and error analysis scheme for DSE DRCs, as well as a simple charge traffic model that simulates DSE DRCs. The equations for our DSE regression and error analysis scheme are extensions of those of Berger (2010) for the E+L model. Using the nomenclature of Berger (2010), the DSE model is

$$f = a(1-e^{-bx}) + c(1-e^{-dx}) \qquad (1)$$

where the second SSE could manifest a second set of charge traps having a different saturation level than the type of traps represented in the first SSE. The

essential equations are outlined below. We illustrate the results with two fine-grain-quartz SAR data sets.

Regression to Obtain Parameters *a, b, c* and *d*

The nomenclature of Berger (2010) is followed here. Using the weighted least-squares principle, we wish to minimize

$$S = \sum_i w_i(y_i - f_i)^2 \qquad (2)$$

where f is defined by Eq 1 and the weights for each y_i value (L/T, SAR normalized OSL) are $1/\sigma_y^2$, and σ^2 is the absolute error variance in each L/T ratio. Corrected (Berger, 2011) Eq 12 of Berger (2010)

$$\Delta A = \left(\left[\sqrt{W}U\right]^t\left[\sqrt{W}U\right]\right)^{-1}\left(\left[\sqrt{W}U\right]^t\left[\sqrt{W}Y^*\right]\right)$$

for the iterative calculation of the best-fit parameters, is used to derive best-fit parameters θ (*a*, *b*, *c* and *d* herein) by iteration, employing the elements of the matrices $\sqrt{W}U$ and $\sqrt{W}Y^*$, where matrix elements $u_{ik} = \partial f_i/\partial\theta_k$. The elements of the weighted matrices are as follows:

$wu_a = (1 - e^{-bx_i})\sqrt{w_i}$,

$wu_b = ax_ie^{-bx_i}\sqrt{w_i}$,

$wu_c = (1 - e^{-dx_i})\sqrt{w_i}$,

$wu_d = cx_ie^{-dx_i}\sqrt{w_i}$,

$wy^* = [y_i - a(1 - e^{-bx_i}) - c(1 - e^{-dx_i})]\sqrt{w_i}$.

Solution for D_e and Error in D_e

We solve for D_e by using the Newton-Raphson iterative procedure (e.g. McCalla, 1967) applied to the equation

$$f' = y_0 - a(1-e^{-bx}) - c(1-e^{-dx}) \qquad (3)$$

because f ' = 0 when x = D_e , where $y_0 = L_0/T_0$, the L/T ratio for the 'natural' measurement.

As in Berger (2010), we calculate two components of the variance in D_e. The first arises from the variance in y_0 and is obtained by using the repeated steps of Berger (2010) and his equation 16

$$\sigma^2_{D_e}(y_0) = \left[\left(D'_e - D''_e\right)/2\right]^2$$

The second error component in D_e arises from the scatter of data about the best-fit curve and from the errors in the parameters *a*, *b*, *c*, and *d*, as well as from the covariances of these errors. We calculate this second component by use of an extension to equation 4 of Berger (1990). This equation is

$$\Delta^2 = \frac{V^t \cdot SIG \cdot V}{|\partial f/\partial D_e|^2},$$

where SIG is the symmetric error matrix (the variance-covariance matrix) and equals $VAR\cdot(I)^{-1}$, I is the information matrix of Berger et al. (1987), and VAR is a scalar.

$$VAR = \frac{\sum_i w_i(y_i - f_i)^2}{N-5}$$

where N is the number of L/T data points including the origin.

Thus, in the equation for Δ^2, $\frac{\partial f}{\partial D_e} = (abe^{-bD_e} + cde^{-dD_e})$, with f given by Eq 1 above. The elements of the above transpose matrix $V^t = (\partial f/\partial a\ , \partial f/\partial b\ , \partial f/\partial c\ , \partial f/\partial d\ )$ are then as follows:

$$\frac{\partial f}{\partial a} = (1 - e^{-bx}),$$
$$\frac{\partial f}{\partial b} = axe^{-bx},$$
$$\frac{\partial f}{\partial c} = (1 - e^{-dx}),$$
$$\frac{\partial f}{\partial d} = cxe^{-dx},$$

and are evaluated with x = D_e.

To complete our calculation of the second component of the error in D_e (that arising from the scatter of data about the best-fit DRC and errors in fitting parameters), we need the elements of the above symmetric matrix I. These elements are derived from Eq 3 of Berger (2010)

$$I_{k,s} = \sum_i \frac{1}{f_i^2}\frac{\partial(f_i)}{\partial\theta_k}\cdot\frac{\partial(f_i)}{\partial\theta_s}$$

and are as follows (with $1/f_i^2$ replaced by w_i as in Berger, 2010):

$I_{aa} = \sum_i w_i(1 - e^{-bx_i})^2$,

$I_{ab} = I_{ba} = \sum_i w_i(1 - e^{-bx_i})(ax_ie^{-bx_i})$,

$I_{ac} = I_{ca} = \sum_i w_i(1 - e^{-bx_i})(1 - e^{-dx_i})$,

$I_{ad} = I_{da} = \sum_i w_i(1 - e^{-bx_i})(cx_ie^{-dx_i})$,

$I_{bb} = \sum_i w_i(ax_ie^{-bx_i})^2$,

$I_{bc} = I_{cb} = \sum_i w_i(ax_ie^{-bx_i})(1 - e^{-dx_i})$,

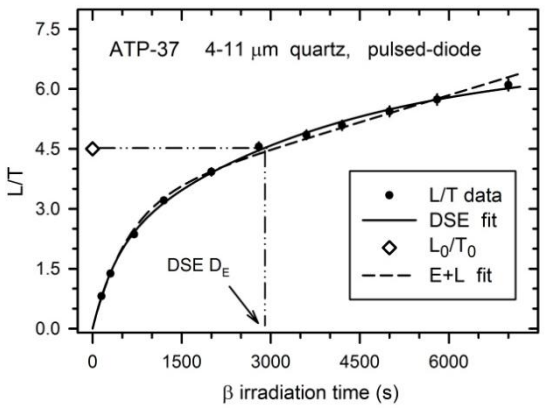

Figure 1: *Comparison of DSE and E+L best-fit DRCs for sample ATP-37. Error bars for L/T data here and in Fig. 2 are ±1σ. Here and for sample ATP-18, a preheat of 240°C(10s) was employed. The dose rate for the beta source used is 0.12 Gy/s.*

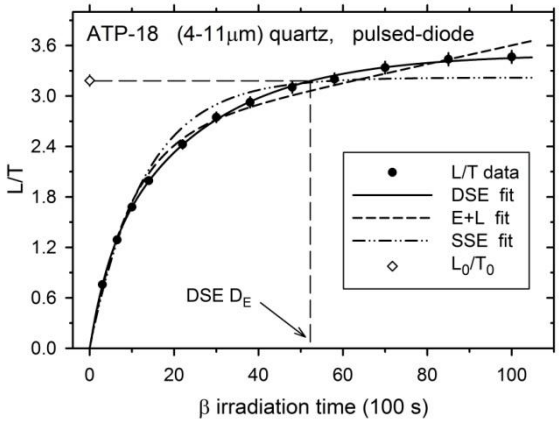

Figure 2: *Comparison of SSE, E+L and DSE best fit DRCs for sample ATP-18. The dose rate of the beta source used is 0.12 Gy/s.*

$I_{bd} = I_{db} = \sum_i w_i(a x_i e^{-b x_i})(c x_i e^{-d x_i})$,

$I_{cc} = \sum_i w_i(1 - e^{-d x_i})^2$,

$I_{cd} = I_{dc} = \sum_i w_i(1 - e^{-d x_i})(c x_i e^{-d x_i})$,

$I_{dd} = \sum_i w_i(c x_i e^{-d x_i})^2$.

The two calculated components of the variance in D_e are then summed as in Eq 15 of Berger (2010) to yield the total variance in D_e.

$$\sigma^2_{D_e} = \sigma^2_{D_e}(y_0) + \sigma^2_{D_e}(\theta)$$

Comparison of Results from Data Sets

The DRC for the data set ATP-37 of Berger (2010) showed an apparently near linear component superimposed upon an SSE. The top of Berger's (2010) Fig. 2 compared the best-fit SSE with the best-fit E+L regressions. In Fig. 1 here we use the same data set to compare the E+L and DSE fits to this high-dose data set. While the differences in the DRCs might appear slight to the eye, they are significant. The 'Fit' value (weighted sums of squares of residuals) for the E+L fit is 1.42, and that for the DSE (0.80) is significantly smaller. Such a Fit value provides a more discriminating estimate of the fit of a regression model than does the less sensitive R^2 value often cited by authors. In this example, the estimated D_e from the DSE regression is smaller (2860 ±190 s) than that from the E+L regression (3060±260 s) as expected, though not statistically different at 1σ.

Table 1: *SAR data for sample ATP-18*

Dose (s)	L/T
Natural	3.184 ± 0.068
300	0.757 ± 0.016
650	1.290 ± 0.028
1000	1.679 ± 0.036
1400	1.994 ± 0.043
2200	2.425 ± 0.052
3000	2.747 ± 0.059
3800	2.925 ± 0.063
4800	3.103 ± 0.067
5800	3.201 ± 0.069
7000	3.338 ± 0.074
8500	3.437 ± 0.074
10000	3.465 ± 0.074
recup'n	0.005 ± 0.002
Recycle	0.84 ± 0.03

Note: These L/T ratios are from the screen display of *Analyst* v3.24, which truncates errors to the third decimal place.

Our second high dose data set (sample ATP-18, Table 1) is also from a 4-11 μm fraction of purified quartz (extracted using H_2SiF_6 acid), apparently having (as does sample ATP-37) only a fast component of quartz OSL. In Fig. 2 we compare the best fit regression curves of SSE, E+L and DSE for the ATP-18 data. Clearly, the SSE model is inappropriate. The SSE Fit value is 3.08. The E+L model evidently provides a better fit, having a Fit value of 1.69, and yielding a D_e value of 6280±700 s.

However, the DSE model provides the closest fit (Fit = 0.40), and the D_e value is smaller (5270±550 s) as expected, with a smaller error. It is clear that a DSE model is more appropriate for these data than is an E+L model, though the error analysis reveals that the difference in estimates of D_e values is not statistically significant at 1σ for these data.

A Charge-traffic Model for a DSE Dose Response

One of the conceptual problems with the use of the E+L regression model is that, although it can represent a realistic physical process under application of high laboratory doses (trap creation superimposed upon filling of existing charge traps, Berger (2010) and citations therein), it is difficult to understand how this model can represent what occurs naturally over geological time scales under much lower dose rates. Notwithstanding, Lowick and Preusser (2011, pg.40) found no empirical evidence in their experiments "to suggest that the presence of a high dose linear response in quartz OSL is only a laboratory generated phenomenon and does not occur in the natural environment". In general, however, several authors (cited in the introduction above) have assumed that a DSE model is more physically realistic, but that in most cases an E+L model provides sufficiently accurate estimates of D_e values from the high dose region of the DRC (and our example data do not show otherwise, at the 1σ level of significance). A particular difficulty has been in conceptualizing a specific charge traffic process or set of competing processes that could account for a DSE dose response.

One envisioned process (e.g. Wintle and Murray, 2006) is that the second SSE term in Eq 1 above manifests the filling of a set of traps different from those manifested by the first SSE term. But what is meant by 'different', and what other charge transport processes might account for such DRCs? Ankjærgaard et al. (2006) provided experimental evidence for discrimination among possible charge traffic schemes of OSL (and TL). They employed optically stimulated electron emission (OSE) and OSL in a comparative study of some natural dosimeters (NaCl, quartz and feldspar). Whereas OSL (and TL) manifest the end results of both charge eviction and charge recombination, OSE reflects only charge eviction. They observed that OSE from quartz and feldspar decays more quickly than OSL, and suggested that this difference manifests the recombination step, possibly involving a delay in the recombination process of OSL (and TL). They also observed differences in the OSE and OSL DRCs, which they attribute to "a dose dependent change in luminescence recombination efficiency", associated

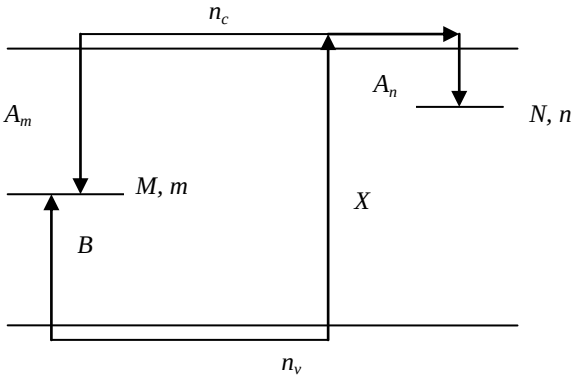

Figure 3: *Charge traffic model used in this study.*

with OSL. However, Ankjærgaard et al. (2009) observed no significant differences in DRC shapes resulting from similar OSE and OSL experiments on additional quartz samples, inferring that luminescence recombination is not generally the main limit to the dose range of DRCs. Furthermore, Lowick et al. (2010a, p. 983) inferred from their experiments with quartz OSL that the high dose behaviour in the DRC could be accounted for by "a change in competition for electrons between the UV recombination centres whose emission is seen through the detection window and recombination centres that do not emit in this spectral region...".

In the context of the above, we present a simple charge traffic model that produces statistically good DSE DRCs, but that involves only one electron trapping state (*N*) and one type of recombination centre (*M*), and (significantly) a 'long' relaxation time. The model is sketched in Fig. 3. Parameters *N* (cm^{-3}) and *M* (cm^{-3}) denote the concentrations of the traps and centres, respectively, and *n* (cm^{-3}) and *m* (cm^{-3}) their corresponding instantaneous occupancies. The parameters n_c (cm^{-3}) and n_v (cm^{-3}) are the instantaneous concentrations of free electrons and holes, respectively. Parameter *B* (cm^3s^{-1}) is the probability coefficient for capturing free holes in the recombination centre. Parameter A_m (cm^3s^{-1}) is the recombination probability coefficient for electrons to recombine with holes in the centres, and A_n (cm^3s^{-1}) the probability coefficient for retrapping. Parameter *X* ($cm^{-3}s^{-1}$) is the rate of production of electron-hole pairs by the irradiation, which is proportional to the excitation dose rate. If an excitation of constant intensity takes place for a period of time t_D (s), the total number of pairs produced is $X \cdot t_D$ (cm^{-3}), which is proportional to the total applied dose *D*.

The set of rate equations governing the process is:

$$\frac{\mathrm{dn}}{\mathrm{dt}} = A_n(N-n)n_c \qquad (4)$$

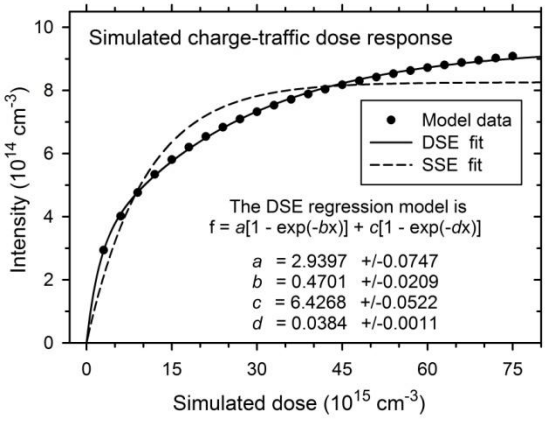

Figure 4: *Simulated charge traffic dose response and best fit regressions. These regressions (from SigmaPlot v11.2) use $1/y^2$ weighting.*

$$\frac{\mathrm{dm}}{\mathrm{dt}} = B(M-m)n_v - A_m m n_c \qquad (5)$$

$$\frac{\mathrm{dn_v}}{\mathrm{dt}} = X - B(M-m)n_v \qquad (6)$$

$$\frac{\mathrm{dn_c}}{\mathrm{dt}} = \frac{\mathrm{dm}}{\mathrm{dt}} + \frac{\mathrm{dn_v}}{\mathrm{dt}} - \frac{\mathrm{dn}}{\mathrm{dt}} \qquad (7)$$

In order to demonstrate the behaviour of the dependence of excitation on the dose, we have chosen the following set of parameters: $N=10^{15}$ cm^{-3}; $M=10^{16}$ cm^{-3}; $n_0=m_0=0$; $B=10^{-9}$cm^{3}s^{-1}; $A_n=2\times10^{-9}$ cm^{3}s^{-1}; $A_m=10^{-7}$cm^{3}s^{-1} and $X=3\times10^{15}$cm^{-3}s^{-1}. The simulated irradiations had varying lengths between 3 and 75 s, which produced the different 'applied' doses.

In order to simulate the excitation process properly, each excitation was followed by a long relaxation time during which, the remaining holes in the valence band were captured in the recombination centre. The remaining electrons in the conduction band were either retrapped or recombined with holes in the centre during the relaxation time. The final concentrations of electrons following excitation and relaxation were recorded. Note that in this simple model of one trap and one recombination centre, the concentrations of electrons in the trap and holes in the centre must be equal at the end of the relaxation time.

The recorded values of the final trap occupancy are assumed to represent the luminescence signal. In the case of TL, this represents the area under the glow peak measured following the excitation and relaxation. For OSL it represents the integral under the decay curve, again, following excitation and relaxation.

The results of the simulation with the above mentioned set of parameters are shown in Fig. 4. The analysis shows that the DSE regression model yields significantly better agreement with the simulated results than does the single saturating exponential (SSE) model. The exponential constants *b* and *d* in the regression model (Eq 1) seem to be associated with the processes of electron capture in traps (probability coefficient A_n) and of holes in centres (probability coefficient *B*) during the excitation and relaxation.

Conclusions

A scheme for regression and estimation of total variance in paleodose (D_e) values derived from SAR OSL experiments is presented for a double saturating exponential (DSE) dose response curve (DRC). With real SAR data from two samples of fine-silt quartz given relatively high laboratory doses, the DSE regression model provides a better fit to the DRCs than does the saturating exponential plus linear (E+L) regression model. Additionally, the estimated errors in the respective D_e values are smaller (as expected because of the better regression fits) than otherwise. The implication of the DSE behaviour of real sample data for OSL dating by SAR is that there is an upper limit to the OSL of the DRCs and this provides one constraint on the maximum age for such dating that would not be encountered if an E+L model represented actual dose response in nature. The upper age limit is likely constrained by the behaviour represented by the second SSE, which may be related to hole-capture behaviour.

Our simple charge traffic model simulates closely a DSE dose response. This simple model has only a single electron trapping state and a single type of recombination centre, and incorporates a 'long' relaxation time as per the experimental procedure. While this simple charge traffic model appears to provide a sufficient match to the observed best-fit DSE regression, other more complicated charge traffic models might also produce similar results. Nonetheless, the two exponents in our simple model may be associated with the two processes of filling of traps and centres, but the full process is likely to be more complicated.

Acknowledgements

Constructive review comments on the first draft of this manuscript were provided by Prof. Frank Preusser.

References

Ankjærgaard, C., Murray, A.S., Denby, P.M., Bøtter-Jensen, L. (2006) Measurement of optically and thermally stimulated electron emission from natural minerals. *Radiation Measurements* **41**, 780-786.

Ankjærgaard, C., Murray, A. S., Denby, P. M., Jain, M. (2009). Using optically stimulated electrons from quartz for the estimation of natural doses. *Radiation Measurements* **44**, 232-238.

Berger, G.W. (1990) Regression and error analysis for a saturating-exponential-plus-linear model. *Ancient TL* **8**, 23-25.

Berger, G.W. (2010) Estimating the error in equivalent dose values obtained from SAR. *Ancient TL* **28**, 55-66.

Berger, G.W. (2011) Errata: Estimating the error in equivalent dose values obtained from SAR. *Ancient TL* **29**, 51.

Berger, G.W., Lockhart, R.A., Kuo, J. (1987) Regression and error analysis applied to the dose response curves in thermoluminescence dating. *Nuclear Tracks and Radiation Measurements* **13**, 177-184.

Bøtter-Jensen, L., McKeever, S. W. S., Wintle, A. G. (2003). *Optically Stimulated Luminescence Dosimetry*. Elsevier.

Lowick, S.E., Preusser, F. (2011) Investigating age underestimation in the high dose region of optically stimulated luminescence using fine grain quartz. *Quaternary Geochronology* **6**, 33-41.

Lowick, S.E., Preusser, F., Wintle, A.G. (2010a) Investigating quartz optically stimulated luminescence dose-response curves at high doses. *Radiation Measurements* **45**, 975-984.

Lowick, S.E., Preusser, F., Pini, R., Ravazzi, C. (2010b) Underestimation of fine grain quartz OSL dating towards the Eemian: comparison with palynostratigraphy from Azzano Decimo, northeastern Italy. *Quaternary Geochronology* **5**, 583-590.

McCalla, T.R. (1967) *Introduction to Numerical methods and FORTRAN Programming*. John Wiley & Sons, New York, 351pp.

Murray, A. S., Svendsen, J. I., Mangerud, J., Astakhov, V. I. (2007) Testing the accuracy of quartz OSL dating using a known-age Eemian site on the river Sula, northern Russia. *Quaternary Geochronology* **2**, 102-109.

Murray, A. S., Buylaert, J-P., Henriksen, M., Svendsen, J-I., Mangerud, J. (2008) Testing the reliability of quartz OSL ages beyond the Eemian. *Radiation Measurements* **43**, 776-780.

Pawley, S.M., Bailey, R.M., Rose, J., Moorlock, B.S.P., Hamblin, R.J.O., Booth, S.J., Lee, J.R. (2008) Age limits on Middle Pleistocene glacial sediments from OSL dating, north Norfolk, UK. *Quaternary Science Reviews* **27**, 1363-1377.

Pawley, S.M., Toms, P., Armitage, S.J., Rose, J. (2010) Quartz luminescence dating of Anglian Stage (MIS 12) fluvial sediments: comparison of SAR age estimates to the terrace chronology of the Middle Thames valley, UK. *Quaternary Geochronology* **5**, 569-582.

Timar, A., Vandenberghe, D., Panaiotu, E.C., Panaiotu, C.G., Necula, C., Cosma, C., van den Haute, P. (2010) Optical dating of Romanian loess using fine-grained quartz. *Quaternary Geochronology* **5**, 143-148.

Wintle, A. G., Murray, A. S. (2006) A review of quartz optically stimulated luminescence characteristics and their relevance in single-aliquot regeneration dating protocols. *Radiation Measurements* **41**, 369-391.

Reviewer

F. Preusser